Perturbation Stability of Frictional Sliding with Varying Normal Force[1]

Pierre E. Dupont Deepak Bapna
ASME, Associate Member
Aerospace and Mechanical Engineering
Boston University
Boston MA 02215

Abstract

In many systems, the normal force at friction contacts is not constant, but instead is a function of the system's state variables. Examples include machine tools, friction dampers, brake systems and robotic contact with the environment. Friction at these contacts has been shown to possess dynamics associated with changes in normal force. In an earlier paper, the authors derived a critical value of system stiffness for stability based on a linearized analysis of constant velocity sliding (Dupont and Bapna, 1994). In this paper, the domain of attraction for the steady sliding equilibrium point is characterized for a system in which normal force is coupled to tangential displacement. Perturbations consisting of sudden changes in the position and velocity of the loading point are considered. These perturbations can be viewed as either actuator disturbances or changes in control input. The effect and interaction of the frictional and geometric parameters are elucidated. The results are applicable to the design and analysis of systems in which steady motion without friction-induced limit cycles is desired.

1 Introduction

Most mechanical systems include friction interfaces and are of finite stiffness. As a result, the potential exists for unsteady motion which is usually detrimental to performance. In precision machining applications, for example, friction within the machine can produce unsteady tool motion which affects the shape of the machined parts (Yang and Tomizuka, 1988). In addition, friction between the tool and workpiece can lead to chatter which is manifested in waviness of the workpiece's surface (Prakash and Clifton, 1992; Ibrahim, 1994). In brake systems as well, considerable effort is devoted to the elimination of brake noise arising from chatter and squeal (Ibrahim, 1994).

[1]This work was supported in part by the National Science Foundation under grant MSS-9302190.

Nomenclature

A	=	parameter expressing dependence of friction on current velocity
B	=	parameter expressing dependence of friction on prior values of velocity and average normal stress
g	=	dimensionless average friction shear stress
k	=	spring constant
k_{cr}	=	critical spring constant
L	=	characteristic sliding distance
M_g	=	maximum overshoot in g
M_ϕ	=	maximum overshoot in ϕ
P_ϕ	=	instantaneous change in ϕ due to a load-point position perturbation
t	=	time
v	=	block velocity
v_0	=	load-point velocity
(v_*, μ_*)	=	reference values of velocity and steady-state friction coefficient
$x, \dot{x}$	=	perturbations from steady-state displacement and velocity
x_0	=	displacement of load point
α	=	evolutionary component of steady-state friction coefficient
δ	=	displacement of block
μ	=	friction coefficient
μ_{ss}	=	steady state friction coefficient
ϕ	=	natural logarithm of dimensionless velocity
ψ	=	spring angle
σ	=	average normal (bearing) stress
σ_0	=	nominal normal stress
σ_{ss}	=	steady-state normal stress
τ	=	average friction shear stress
θ	=	friction state variable

As another example, dry friction dampers and fasteners are used to dissipate vibrational energy in turbine blades, aircraft frames and large space structures (Anderson and Ferri, 1990; Ferri and Bindemann, 1992; Ferri and Heck, 1992). Dampers in which normal force increases with tangential displacement have been shown to possess viscous-like damping properties (Anderson and Ferri, 1990). Here too, steady motion (minimal sticking) is desired in order to maximize energy dissipation (Ferri and Bindemann, 1992).

The literature on techniques for the design and analysis of systems with friction is large (Armstrong-Hélouvry et al., 1994; Ibrahim, 1994). All methods involve approximations of the actual system and perhaps the most important approximation in this case is the choice of friction model. A majority of the literature on frictional instabilities employs friction models in which normal force is constant (Armstrong-Hélouvry et al., 1994). In all of the applications mentioned above, however, there exists coupling between the normal force at the friction interface and other forces or displacements in the system.

The relevance of friction dynamics has only recently been recognized and experimentally-tested dynamic friction models have not been widely available (Armstrong-Hélouvry, 1993; Dupont and Dunlap, 1995). Consequently, those papers that do treat varying normal force have typically assumed that the frictional dependence is linear (Ibrahim, 1994).

Several papers have addressed the existence and modeling of frictional dynamics associated with normal force (Hobbs and Brady, 1985; Lockner et al., 1986; Linker and Dieterich, 1992). Two other papers, (Dieterich and Linker, 1992; Dupont and Bapna, 1994), have developed linearized stability criteria for steady sliding motion of systems subject to the dynamic friction law proposed in (Linker and Dieterich, 1992). Since the friction law is nonlinear, however, the linearized stability criteria apply for small perturbations of unknown magnitude.

In this paper, we address the question of how the geometry and the load-dependent friction properties of a system affect its ability to reject disturbances and track commanded inputs. We do so for one important geometry in which normal force is coupled by system stiffness to displacement at the friction interface. We employ the friction model of (Linker and Dieterich, 1992) which is applicable for the low velocities and small displacements of boundary lubrication. While friction can differ between systems, the qualitative trends of this model could provide insights regarding

the behavior of other friction models. A Coulomb-like instantaneous response to changes in normal force is a limiting case of this model.

The paper is arranged as follows. In the next section, the friction model is defined and its response to changes in normal force and velocity are described. In section 3, the system geometry under consideration is presented and its governing equations are derived. In section 4, the stability of perturbations to steady sliding is studied in the phase plane. The domains of attraction are considered for step changes in load-point position and velocity. The effects of frictional and geometric parameters on transient response are summarized. The case of zero load-point velocity is also considered. The paper concludes with a summary of design guidelines for systems of this type.

2 Friction Model

It is often observed experimentally that friction cannot be represented by an algebraic equation relating system state variables (e.g., sliding velocity) to friction force. Rather, the friction force itself possesses dynamics (Armstrong-Hélouvry et al., 1994). During stick slip, this is usually manifested as a higher friction coefficient during the acceleration phase of the slip than during the deceleration phase.

In lubricated contacts at velocities sufficient to eliminate solid to solid contact, it is most likely the fluid film dynamics which control the evolution of friction force (Hess and Soom, 1990; Harnoy et al., 1994). At low velocities under boundary lubrication, it is likely that the evolution of the asperity contacts determines the friction dynamics (Dieterich, 1979; Dieterich and Linker, 1992).

In boundary lubrication, the response to a step change in velocity has been studied experimentally for a variety of materials including steel on steel, teflon on steel, glass, plastic, wood and rock (Dieterich, 1991; Dupont and Dunlap, 1995). The friction force for a step increase in velocity evolves as shown in Figure 1. Depending on the materials and lubricant, there may be an instantaneous viscous effect of magnitude A. This is followed by an exponential decay of magnitude B to the final steady-state friction level associated with $v_0 + \Delta v$. (In the model which follows, the changes in friction stress denoted by A and B correspond to the velocity step, $\Delta v = (e-1)v_0$ where $e = 2.71828....$) For those materials tested, this decay appears to occur over characteristic sliding

distances (Dieterich, 1991; Dupont and Dunlap, 1995)

Several researchers have studied the transient behavior of friction in response to changes in normal force (Hobbs and Brady, 1985; Lockner et al., 1986; Linker and Dieterich, 1992). All observed that a sudden increase (decrease) in normal force causes a sudden increase (decrease) in friction and an evolutionary increase (decrease) in friction to a new steady-state level as sliding proceeds. The response for a step increase in normal stress is depicted in Figure 2. The evolutionary component of the response is given by $\alpha\ \Delta\sigma$ while the instantaneous component is $(\mu_{ss} - \alpha)\Delta\sigma$.

Linker and Dieterich (1992) proposed the following model which has been used in several papers to study the stability of systems with varying normal force (Dieterich and Linker, 1992; Dupont and Bapna, 1994).

$$\tau = \sigma \left[\mu_* + A \ln \left(\frac{v}{v_*} \right) + B\theta \right] \tag{1}$$

$$\dot{\theta} = -\frac{v}{L} \left[\ln \left(\frac{v}{v_*} \right) + \theta \right] - \frac{\alpha}{B\sigma} \dot{\sigma} \tag{2}$$

To be consistent with the notation of earlier papers, the friction law is written in terms of normal stress, σ, and friction shear stress, τ. The reader should understand that these are average quantities which refer to the normal and friction forces divided by apparent area of contact.

In this equation, θ is a frictional state variable while A, B and α are as shown in Figures 1 and 2. μ_* is the steady state coefficient of friction at the reference velocity, v_*. L is the characteristic sliding distance controlling the evolutionary response to changes in both velocity and normal stress. This model is used in the remainder of the paper.

For the case of constant normal stress, Dieterich (1979) provides a physical interpretation of the state variable. He proposes that θ is proportional to the apparent age of the asperity junctions. When normal stress can vary, Linker and Dieterich (1992) propose that θ is related to the fraction of the contact area associated with time-dependent creep.

3 Inclined-Spring System

An important case of coupling between normal force and a system's state variables occurs when the friction forces are borne by an elastic member whose normal and tangential displacements are dependent. Consider a block of unit base area, pulled by a spring of stiffness k at an angle ψ as shown in Figure 3. The free end of the spring is pulled at velocity $v_0 = \dot{x}_0$ while the block slides at velocity $v = \dot{\delta}$. When the spring is relaxed, the normal force is given by σ_0. To be consistent with previous literature, the free end of the spring will be called the load point. In an actuated system, the load-point velocity $v_0 = \dot{x}_0$ can be viewed as the control input. In other applications (e.g., brakes), it may be appropriate, through kinematic inversion, to view the load point as held stationary by a constraint force while the surface under the block is in motion.

This model applies to a number of practical situations. For example, the pressure shear impact tests of Clifton for the study of machine tool/workpiece interface friction can be modeled in this way (Prakash and Clifton, 1992). A similar apparatus is used by geologists to study rock friction (Dieterich and Linker, 1992). In many brake systems as well, the brake pad is forced against the rotor by means of a lever arm at a nominal angle ψ (Ibrahim, 1994).

Robots using hybrid position/force control to perform mechanical assembly and other operations also conform to this model. In addition, by taking $\psi = 0$, systems with a normal force which is nominally constant, but may vary due to disturbance forces can be modeled. For example, the compensation of friction in machine tool slideways subject to normal force perturbations arising from varying cutting forces can be studied.

Dry friction dampers for turbine blades and large space structures may be similarly modeled, however, the equilibrium velocity for dampers is zero (Anderson and Ferri, 1990; Ferri and Bindemann, 1992; Ferri and Heck, 1992).

The normal stress, σ, is given by

$$\sigma = \sigma_0 + k \tan\psi(\delta - x_0) \tag{3}$$

where δ and x_0 are the displacement of the block and load point, respectively. Let

$$\delta = x_{ss} + x$$

so that x represents the shortening of the spring from the its steady-state length.

At steady-state

$$\sigma_{ss} = \sigma_0 + k \tan\psi (x_{ss} - x_0) \tag{4}$$

From (3) and (4), normal stress can be written as

$$\sigma = \sigma_{ss} + kx \tan\psi \tag{5}$$

As shown in (Dupont and Bapna, 1994), quasistatic analysis was found to be a good approximation to the inertial system for a wide range of masses, particularly for the case of $\tan\psi < 0$.

In the equations which follow, τ_{ss}, σ_{ss}, and μ_{ss} represent the steady-state values of friction stress, normal stress and friction coefficient for a load-point velocity of v_0.

For the quasistatic case (i.e., when $m\ddot{\delta}$ is small relative to the other terms),

$$\tau = -k(\delta - x_0) \tag{6}$$

We introduce dimensionless coordinates for velocity and shear stress given by

$$\phi = \ln\left(\frac{v}{v_0}\right) \tag{7}$$

and

$$g = \frac{\tau - \tau_{ss}}{\sigma_{ss}}, \tag{8}$$

respectively. Combining equations (1),(2),(3) and (6), the quasistatic motion of the system is described by

$$\begin{aligned}
\dot{g} &= \frac{k v_0}{\sigma_{ss}}(1 - e^{\phi}) \\
\dot{\phi} &= \frac{k v_0 (1 - e^{\phi})}{A\sigma_{ss}(1 - \tan\psi g)}\left[\frac{1 + \tan\psi\ \mu_{ss}}{1 - \tan\psi g} - \tan\psi\alpha\right] \\
&\quad + \frac{v_0 e^{\phi}}{AL}\left[\frac{(1 + \tan\psi\ \mu_{ss})g}{1 - \tan\psi g} + (B - A)\phi\right]
\end{aligned} \tag{9}$$

Dividing the second equation by the first yields

$$\frac{d\phi}{dg} = \frac{1}{A(1-\tan\psi g)}\left[\frac{1+\tan\psi\ \mu_{ss}}{1-\tan\psi g} - \tan\psi\alpha\right] + \frac{\sigma_{ss}}{kAL}\left(\frac{e^{\phi}}{1-e^{\phi}}\right)\left[\frac{(1+\tan\psi\ \mu_{ss})g}{1-\tan\psi g} + (B-A)\phi\right] \tag{10}$$

Equation 10 describes phase plane trajectories for the quasistatic motion of the inclined-spring system with the state variable law given by (1,2) and the normal stress given by (3).

Trajectories were obtained numerically using a fourth-order, variable-step-size, Runge-Kutta method. The trajectories were generated by switching between (9) and (10). Equation 10 was used for $\phi > 0.3$ while (9) was used otherwise. This switching was required due to the limitations of the integration routine.

3.1 Stationary Load Point, $v_0 = 0$

Consider the special case when the system is initially in motion and the load point is suddenly brought to rest. It is possible to obtain an analytic solution for this case given by

$$\frac{d\phi}{dg} = \frac{1}{A(1-\tan\psi g)}\left[\frac{1+\tan\psi\ \mu_{*}}{1-\tan\psi g} - \tan\psi\alpha\right] + \frac{\sigma_{*}}{AkL}\left[\frac{(1+\tan\psi\ \mu_{*})g}{1-\tan\psi g} + (B-A)\phi\right]. \tag{11}$$

This equation is written in terms of μ_* and σ_* to emphasize that the initial and steady state velocities are different.

Defining

$$\gamma = \left(\frac{B-A}{A}\right)\frac{\sigma_{*}}{kL},$$

equation (11) then reduces to

$$\frac{d\phi}{dg} + \gamma\phi = \frac{1+\tan\psi\ \mu_{*}}{A(1-\tan\psi g)^2} - \frac{\tan\psi\alpha}{A(1-\tan\psi g)} - \frac{\sigma_{*}(1+\tan\psi\ \mu_{*})}{AkL}\left(\frac{g}{1-\tan\psi g}\right). \tag{12}$$

By substituting $\tan\psi = \alpha = 0$ in (12), the differential equation describing the case of constant normal stress can be obtained. The result is equivalent to that of Gu et al. (1984).

Solving (12), we find

$$\phi \;=\; ce^{-\gamma g} + \frac{1+\tan\psi\ \mu_{*}}{A\tan\psi}\left(\frac{1}{1-\tan\psi g} + \frac{A}{B-A}\right)$$

$$+\frac{e^{-\gamma(g-\frac{1}{\tan\psi})}}{A}\left\{\frac{1+\tan\psi\ \mu_*}{\tan\psi^2}\left(\gamma+\frac{\sigma_*}{kL}\right)+\alpha\right\}$$

$$\times\left[\ln(1-\tan\psi g)+\sum_{n=1}^{\infty}\frac{\{\frac{-\gamma}{\tan\psi}(1-\tan\psi g)\}^n}{n\times n!}\right] \tag{13}$$

The convergence of the series in (13) follows from the ratio test.

A necessary condition for contact between the block and surface is that the term $(1-\tan\psi g)$, which appears in the equation above, be positive. This follows because we can express σ as

$$\sigma=\sigma_*(1-\tan\psi g) \tag{14}$$

In the context of the inclined-spring model, this means that the block may leave the surface if the spring is stretched too much when it is pulling the block out of the surface or if it is compressed too much while pulling the block into the surface.

For both a moving and stationary load point, the following values from (Linker and Dieterich, 1992) were used to generate the trajectories depicted in the remainder of the paper.

$$A=0.0145, \qquad B=0.0160, \quad L=10^{-6}\text{m}$$

$$\sigma_0=5\times10^6 N/m^2, \quad \mu_{ss}=0.7, \qquad \alpha=0.56$$

4 Perturbations

Previously, two necessary conditions for steady sliding at constant velocity were derived (Dieterich and Linker, 1992; Dupont and Bapna, 1994). The first is that the spring angle, ψ, should lie outside the steady-state friction cone defined by μ_{ss} or

$$1+\mu_{ss}\tan\psi>0. \tag{15}$$

The second, obtained through linearization, indicates the minimum spring stiffness, k_{cr}, necessary for steady sliding. It is given by

$$k_{cr}=\frac{\sigma_{ss}(B-A)}{L\{1+(\mu_{ss}-\alpha)\tan\psi\}} \tag{16}$$

A stiffness equal to k_{cr} produces a limit cycle about the steady sliding equilibrium point. The critical stiffness applies to perturbations from equilibrium of sufficiently small size.

In response to a finite perturbation for $k > k_{cr}$, the system may converge back to steady sliding or it may diverge such that the block sticks or attains a high velocity. This could lead to stick slip. Even if the system does converge to the equilibrium point, it may do so in an undesirable manner.

In this section, we investigate the maximum size of stable perturbations (their domain of attraction) and ascertain the dependence of their transient response on the values of spring stiffness k, steady-state friction coefficient μ_{ss}, frictional lag α, and spring angle ψ. It is assumed that perturbations arise either from disturbance forces which drive the system away from the equilibrium point or from sudden changes in commanded input. An example of the latter would be a step change in commanded velocity requiring the system to move to a new equilibrium point. This could correspond to a desired velocity step or to the staircase output of a digital-to-analog converter.

For the quasistatic inclined-spring system, the phase plane, discussed in the next section, is two dimensional. Any perturbation from the equilibrium point of steady sliding can be decomposed into a combination of steps in the displacement and the velocity of the load point (Gu et al., 1984). The jump to a zero load-point velocity is treated as a separate case. A stationary load point could represent an intentional dwell time or a stiction interval of the actuator.

4.1 Phase Plane

It is convenient to represent the evolution of the system with time on a plane defined by the axes $(\phi, g) = (\ln(\frac{v}{v_0}), \frac{\tau - \tau_{ss}}{\sigma_{ss}})$. In this plane, each point represents a unique combination of velocity and shear strength and has a value of state variable given by (1). The origin represents the steady sliding condition for load-point velocity, v_0. In the phase plane, constant-state curves are straight lines with slope A. The line $\theta = 0$ passes through the origin.

At steady state, $\dot{\theta} = \dot{\sigma} = 0$. From (2), $\theta_{ss} = -\ln(v/v_0)$. Substitution of this value into (1) yields the following equation for the locus of points corresponding to steady sliding for all values of load-point velocity.

$$\phi = \left(\frac{1 + \tan\psi \ \mu_{ss}}{A - B} \right) \frac{g}{1 - \tan\psi g} \tag{17}$$

The steady-state curves for $\psi = \pm\pi/4$ are shown in Figure 4. For constant normal stress, these curves reduce to a line through the origin with slope, $(A - B)$.

One type of perturbation corresponds to a sudden change in the velocity of the load point. Assuming that the system was initially at steady state, this type of perturbation instantaneously moves the equilibrium point to a new position on the steady state curve. The trajectory taken to the new equilibrium point is described by (9).

A second type of perturbation involves a change in shear stress without any change in load-point velocity. This can be caused by a sudden change in load-point displacement. To picture such a perturbation in the phase plane, consider that the evolution equation (2) for θ can be expressed as:

$$d\theta = -\frac{d\delta}{L} \left[\ln\left(\frac{v}{v_0} \right) + \theta \right] - \frac{\alpha}{B\sigma} d\sigma \tag{18}$$

When the load point is suddenly displaced, the block does not move instantaneously and hence $d\delta = 0$. In this case, the equation above simplifies to

$$d\theta = -\frac{\alpha}{B\sigma} d\sigma \tag{19}$$

with

$$d\sigma = -\tan\psi d\tau$$

The shear stress, τ, as given by (1), when expressed in terms of the dimensionless velocity, ϕ becomes

$$\tau = \sigma \left[\mu_{ss} + A\phi + B\theta \right]$$

Differentiation and substitution of expressions for $d\sigma$, $d\theta$ and σ yields the following differential equation for the load-point displacement perturbation curve.

$$\frac{d\phi}{d\tau} = \frac{1}{A} \left[\frac{1 - \alpha \tan\psi}{\sigma_0 - \tan\psi\tau} + \frac{\tan\psi\tau}{(\sigma_0 - \tan\psi\tau)^2} \right] \tag{20}$$

If the system is at (ϕ_1, g_1) when the perturbation occurs, the equation can be integrated to obtain

$$P_\phi = \phi - \phi_1 = \frac{1}{A} \left[\alpha \ln\left(\frac{1 - \tan\psi g}{1 - \tan\psi g_1} \right) + \frac{(1 + \tan\psi \ \mu_{ss})(g - g_1)}{(1 - \tan\psi g_1)(1 - \tan\psi g)} \right] \tag{21}$$

Figure 4 depicts the load-point displacement perturbation curves for two spring angles, $\psi = \pm\pi/4$. For constant normal stress, these curves reduce to a line of constant state, θ, which lies approximately midway between the pair of curves shown.

The figure also illustrates, for each spring angle and initial conditions $(\phi_i, g_i) = (0, 0)$, load-point displacement perturbations and the subsequent response of the system. The perturbation moves the system instantaneously from the origin to point a (a') for $\psi = -\pi/4$ ($\psi = \pi/4$). The ensuing trajectory back to the origin follows a solution to (9). During the perturbation, the increase in ϕ, denoted P_ϕ, for $\psi = \pi/4$ is slightly larger than that of $\psi = -\pi/4$. During the ensuing motion, however, the maximum block velocity for $\psi = \pi/4$ is 2.4 times that for $\psi = -\pi/4$.

As can be seen from this figure, any general perturbation from the origin (initial condition in the phase plane) can be decomposed into perturbations in load-point displacement and velocity. In addition, certain load point trajectories may be modeled as a sequence of perturbations.

For example, it may be possible to analyze the effect of the load point undergoing stick slip motion by considering alternating load-point displacement perturbations and periods of a stationary load point. The stick phase may correspond to a stationary load point if the displacement of the load point during stick is small compared to that of the block. The slip phase, if of high velocity and short duration in comparison to block friction dynamics, may be modeled as an instantaneous displacement of the load point.

4.2 Domain of Attraction

The linearized stability result indicates that the origin of the phase plane is stable for spring stiffnesses greater than k_{cr} under sufficiently small perturbations. Given a value of k, the domain of attraction is the set of points in the phase plane for which the nonlinear system converges to the origin (is asymptotically stable).

4.2.1 Moving Load Point

Figure 5 depicts one stable and one unstable trajectory for $\psi = \pi/4$. While no equation for the boundary of the domain of attraction is known, this boundary exists and lies between the stable and unstable trajectories shown in the figure.

Note that stable trajectories near the stability boundary experience very high velocities before reaching equilibrium. To give an illustration, for the stable trajectory shown in Figure 5, ϕ goes as high as 125. The velocity at this point is $e^{125}v_0$ ($= 1.93558 \times 10^{54}v_0$). This is well outside the range of ϕ for which the model is valid. Thus, knowledge of the location of the actual boundary is not necessary.

A more appropriate stability boundary can be defined by prescribing bounds on either shear stress transients or velocity transients or both. Shear stress transients could be important if an actuator is operating near saturation. In precision motion control applications, velocity transients would be of considerable concern.

Suppose, for example, that one is interested in determining the maximum step increase in load-point velocity for which the maximum velocity overshoot of the block does not exceed $\phi = 7$ ($v_{max}/v_{final} = e^7$). Since the system is time invariant, phase plane trajectories do not cross each other. The maximum velocity step can be obtained by starting at the point given by $\phi = 7$, $\partial g/\partial\phi = \infty$ and following the system backwards in time until the steady-state curve is reached. Figure 6 shows the maximum velocity step $\Delta\phi$ as a function of spring stiffness for five spring angles.

4.2.2 Stationary Load Point

When the velocity of the load point is suddenly set to zero, the system will eventually slow down. However, this may be preceded by high block velocities.

Before proceeding to the analysis, we need to note that for the case of a stationary load point, the usual interpretation of k_{cr} is not possible. In this case, the equilibrium is at $\phi = -\infty$ and linearization about $-\infty$ is inappropriate for a nonlinear system. The value of k does determine the domain of attraction and the rate at which the system converges to the equilibrium point.

For constant normal stress, the stability boundary for trajectories described by a simplified (12) is given by a line which, for $k > 0$, intersects the ϕ-axis at a positive value of ϕ (Gu et al., 1984). Velocities along trajectories starting to the right of this line tend toward infinity while those of trajectories to the left of the line tend toward zero (i.e., the block stops). As k increases, this line shifts to the right along the ϕ axis, thus increasing the region in the phase plane where the

trajectories are stable.

In the case of variable normal stress, the phase plane trajectories defined by (13) are depicted in Figure 7 for $\tan\psi = 1$ and various initial conditions. Unlike the constant normal stress case, an equation for the stability boundary is not easily obtained. It can be seen from the figure, however, that there is a boundary separating the stable and unstable trajectories.

As was the case for a moving load point, some trajectories within the domain of attraction, while asymptotically stable, attain high velocities before the system comes to rest. For all practical purposes, these trajectories can be considered unstable. If a maximum allowable velocity is specified, we can find a trajectory such that for all the initial conditions to the left of this trajectory, velocities will always remain less than the maximum allowable velocity. This trajectory will serve as a practical stability boundary.

Setting $\frac{d\phi}{dg} = 0$ in (12) we get

$$\phi = \frac{1}{A\gamma(1-\tan\psi g)}\left\{\frac{1+\tan\psi\ \mu_*}{(1-\tan\psi g)} - \tan\psi\alpha\right\} - \frac{1}{B-A}\left\{\frac{(1+\tan\psi\ \mu_*)g}{1-\tan\psi g}\right\} \tag{22}$$

Once a maximum allowable velocity is chosen, the corresponding g can be calculated from (22) and the trajectory through this point computed. Since the trajectories do not cross each other in the phase plane, this trajectory can be considered the stability boundary.

4.3 Effect of Parameters

Several parameters affect the location of both the actual and transient-limited stability boundaries. These are the stiffness, k, the steady-state coefficient of friction, μ_{ss}, its evolutionary component, α and the spring angle, ψ. Their qualitative effect on transient response is similar for a moving and stationary load point. These effects are summarized in Table 1. As reported in (Bapna, 1992; Dupont and Bapna, 1994), increasing k decreases overshoot in velocity and friction stress. The effect of varying μ_{ss} in the range shown produces little effect for a moving load point.

The effects of μ and ψ on stability and transient response are coupled. Some understanding of their interrelationship can be found by examining the equation for critical stiffness given by (16). Considering first the case of constant normal stress, if friction responded instantaneously to changes in sliding conditions, $L \to 0$ and $k_{cr} \to \infty$. The existence of a finite critical stiffness depends on

	Effect of Increasing Parameter	
Parameter	$v_0 \neq 0$	$v_0 = 0$
α	$\psi > 0$: $M_\phi \uparrow$, $M_g \uparrow$ $\psi < 0$: $M_\phi \downarrow$, $M_g \downarrow$ Position Perturbation: $\{$ $\psi > 0$: $P_\phi \downarrow$; $\psi < 0$: $P_\phi \uparrow$	$\psi > 0$: $M_\phi \uparrow$ $\psi < 0$: $M_\phi \downarrow$
ψ	$k_{cr} \downarrow$ Position Perturbation: $P_\phi \uparrow$, $M_\phi \uparrow$ Velocity Perturbation: $M_\phi \downarrow^*$, $M_g \downarrow$	(No k_{cr}) $M_\phi \uparrow$
k	$M_\phi \downarrow$, $M_g \downarrow$	$M_\phi \downarrow$
μ_{ss}	Effect is small for $\mu_{ss} \in [0.56, 0.70]$	Effect is small

Table 1: Effect of parameters on transient response. M_ϕ and M_g are the maximum overshoot in block velocity and friction stress, respectively. P_ϕ is the instantaneous change in block velocity due to a position perturbation. All perturbations are those of the load point. Note that there is no M_g for $v_0 = 0$. ($\uparrow$= increases, $\downarrow$= decreases, $*$ = for $k/k_{cr}(\psi = \pi/4) < 5.25$).

the existence of frictional lag embodied in the state variable dynamics (2).

Next consider an inclined spring system for which friction responds instantaneously to changes in normal force ($\alpha = 0$). (16) indicates that increasing ψ decreases critical stiffness. This follows since the spring-induced changes in friction force drive the system toward the equilibrium point for $\psi > 0$. For example, when block position falls behind its steady-state position, the stretched spring decreases the normal force and with it the destabilizing friction force. When block position exceeds its steady-state position, the contracted spring increases normal force and with it the stabilizing friction force. The opposite is true for $\psi < 0$.

Now consider a nonzero α which represents the evolutionary component (frictional lag) of the change in friction stress due to a change in normal stress. (Recall $0 \leq \alpha \leq \mu_{ss}$.) As can be seen from (16), increasing α tends to destabilize the system when the spring is pulling the block out of the surface. The lag reduces the stabilizing effect of the positive spring angle, i.e., damping is reduced. The converse is true when the system is pulling the block into the surface. Increasing α delays the destabilizing effect of $\psi < 0$ and the system converges more quickly to the origin.

In summary, for all spring angles, the α lag reduces the effect of the spring angle. This is made clear in Figures 9 and 10 which depict the effect of α on the phase plane trajectories for $\psi = \pm\pi/4$ given a single set of initial conditions. The same holds true for load-point velocity perturbations as the steady-state curve (17) is independent of α. This effect is countered during load-point displacement perturbations, however, by the influence of α on P_ϕ in (21).

Spring angle also affects the shape of the transient trajectory. Plotted on the same axes, positive spring angles produce trajectories which are much flatter in shape compared to those generated from negative angles. Consequently, the maximum overshoot in velocity or friction stress in response to a perturbation depends on whether the perturbation is mainly in the stress or velocity direction.

From Figure 4, note that load-point displacement perturbations follow curves with a steep slope in the phase plane. Conversely, load-point velocity perturbations follow steady-state curves with small negative slopes. As shown by the trajectories depicted in this figure, it is the ψ-dependent trajectory shape which determines the relative velocity overshoot in response to load-point displacement perturbations. Negative spring angles produce smaller maximum velocities. For

the same reason, if the maximum velocity overshoot is specified, negative spring angles allow larger load-point displacement perturbations.

The result is not the same, however, if one considers load-point velocity perturbations as shown in figure 6 (for fixed velocity overshoot). Although increasing ψ produces a flatter trajectory, the rate of convergence (in the velocity direction) is only weakly dependent on ψ for small $k > k_{cr}$. The larger size of the allowable velocity steps for $\psi > 0$ in figure 6 is consequently due primarily to the trend toward a horizontal steady-state curve for increasing ψ. As k increases, however, the relative rate of convergence for negative spring angles increases such that at $k \approx 5.25 k_{cr}(\psi = \pi/4)$, M_ϕ is independent of ψ.

5 Conclusions

Much effort has been devoted to friction compensation (controller design) based on the assumption that the mechanical and frictional properties of the system are fixed. In this vein, the interrelationship of mechanical and frictional parameters revealed in the preceding section does allow for a better understanding and analysis of existing systems. The major motivation for this paper, however, has been to reconsider mechanical design from the viewpoint of producing a system which is easier to control.

If one is designing a system which can be modeled by the inclined-spring system, there a number of factors to consider. The foremost is to ensure that the stiffness exceeds the critical value necessary for steady sliding. Negative spring angles ($\psi < 0$) require stiffer springs for stability and the spring angle must lie outside the friction cone to avoid jamming. If, however, the system is likely to experience load-point position perturbations, (e.g., short periods of rapid load point slip) negative spring angles produce less velocity overshoot.

If load-point velocity perturbations are expected (e.g., velocity step inputs), increasing the spring angle will decrease the velocity overshoot for $k < 5k_{cr}(\pi/4)$. It will also decrease the friction stress overshoot and thus decrease the maximum load borne by the load-point actuator.

Frictional lag associated with changes in normal force can have a significant effect on the transient dynamics as shown in Figures 9 and 10. According to the sign of the selected spring angle, the lag can be either stabilizing or destabilizing. To achieve prescribed performance criteria,

selection of materials, lubricants, spring stiffness and spring angle should be considered concurrently.

While friction does vary from system to system, its basic components, including frictional memory, are the same. Consequently, the results presented here could provide qualitative insight into the design of systems whose frictional nuances might be better represented by a different model. Building on the material presented here, further study could address the issue of assembling arbitrary stable input trajectories from the studied perturbations.

6 References

Anderson, J.R. and Ferri, A.A., 1990, "Behavior of a single-degree of freedom system with a generalized friction law," *Journal of Sound and Vibration*, 140(2):287–304.

Armstrong-Hélouvry, B., 1993, "Stick-slip and control in low-speed motion," *IEEE Trans. on Auto. Control*, 38(10):1483–1496.

Armstrong-Hélouvry, B., Dupont, P, and Canudas de Wit, C., 1994, "A survey of models, analysis tools and compensation methods for the control of machines with friction," *Automatica*, 30(7):1083–1138.

Bapna, D., 1992, "The stability of sliding systems with friction subject to varying normal stress," Master's thesis, Aerospace and Mechanical Engineering, Boston University.

Dieterich, J.H., 1979, "Modeling of rock friction: 1. experimental results and constitutive equations," *Journal of Geophysical Research*, 84:2161–2168.

Dieterich, J.H., 1991, "Micro-mechanics of slip instabilities with rate- and state-dependent friction," *Eos, Trans. Am. Geophys. Union*, Fall Meeting Abstract Volume, p. 324.

Dieterich, J.H. and Linker, M.F., 1992, "Fault stability under conditions of variable normal stress," *Geophysical Research Letters*, 19(16):1691–1694.

Dupont, P. and Bapna, D., 1994, "Stability of sliding frictional surfaces with varying normal force," *ASME J. Vibration and Acoustics*, 116:237–242.

Dupont, P. and Dunlap, E., 1995, "Friction modeling and pd compensation at very low velocities," *ASME Journal of Dynamic Systems, Measurement and Control*, March, to appear.

Ferri, A.A. and Bindemann, A.C., 1992, "Damping and vibration of beams with various types of frictional support conditions," *Journal of Vibration and Acoustics*, 114:289–296.

Ferri, A.A. and Heck, B.S., 1992, "Analytical investigation of damping enhancement using active and passive structural joints," *Journal of Guidance, Control and Dynamics*, 15(5):1258–1264.

Gu, J.C., Rice, J.R., Ruina, A.L., and Tse, S.T., 1984, "Slip motion and stability of a single degree of freedom elastic system with rate and state dependent friction," *J. Mech. Phy. Solids*, 32:167–196.

Harnoy, A., Friedland, B., and Rachoor, H., 1994, "Modeling and simulation of elastic and friction forces in lubricated bearings for precise motion control," *Wear*, 172:155–165.

Hess, D.P., and Soom, A., 1990, "Friction at a lubricated line contact operating at oscillating sliding velocities," *J. of Tribology*, 112(1):147–152.

Hobbs, B., and Brady, B., 1985, "Normal stress changes and the constitutive law for rock friction (abstract)," *Eos trans. AGU*, 66:382.

Ibrahim, R.A., 1994, "Friction-induced vibration, chatter, squeal and chaos part ii: Dynamics and modeling," *Applied Mechanics Reviews*, 47(7):227–253.

Linker, M., and Dieterich, J., 1992, "Effects of variable normal stress on rock friction: Observations and constitutive equations," *Journal of Geophysical Research*, 97(B4):4923–4940.

Lockner, D., Summer, R., and Byerlee, J., 1986, "Effects of temperature and sliding rate on frictional strength of granite," *Pure Appl. Geophys.*, 124:445–485.

Prakash, V., and Clifton, R., 1992, "Pressure-shear plate impact measurement of dynamic friction for high speed machining applications," In *Proc. VII Int. Congress on Exp. Mechanics*, Las Vegas: Soc. Exp. Mechanics, June.

Yang, S., and Tomizuka, M., 1988, "Adaptive pulse width control for precise positioning under the influence of stiction and coulomb friction," *Journal of Dynamic Systems, Measurement and Control*, 110:221–227.

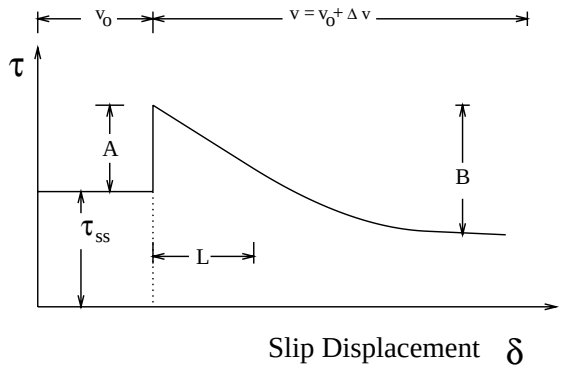

Figure 1: Response of average friction shear stress τ to step change in velocity, Δv.

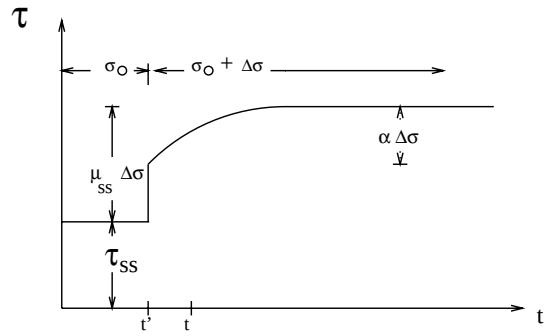

Figure 2: Response of average friction shear stress τ to step change in normal stress, $\Delta\sigma$.

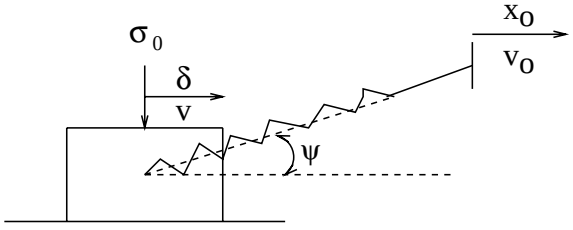

Figure 3: Inclined-Spring model.

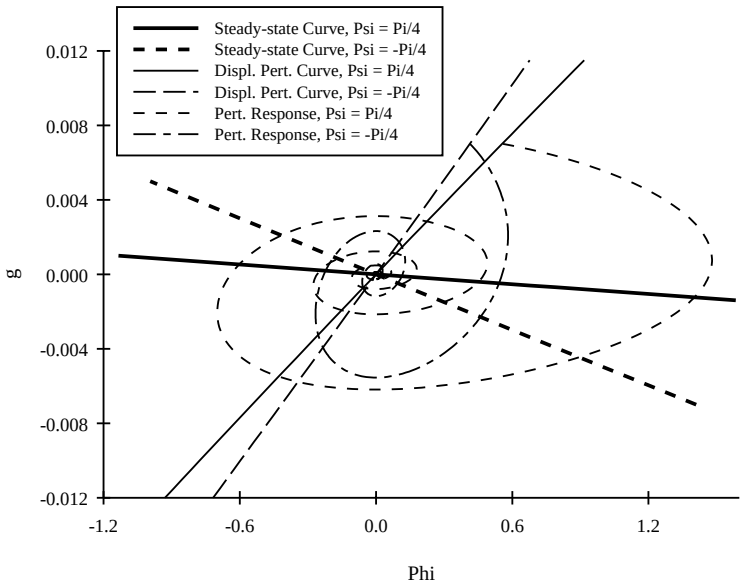

Figure 4: Characteristic Curves for Inclined-Spring Model with $\psi = -\pi/4$ and $\psi = \pi/4$. Trajectories for load-point displacement perturbations are shown for the two spring angles.

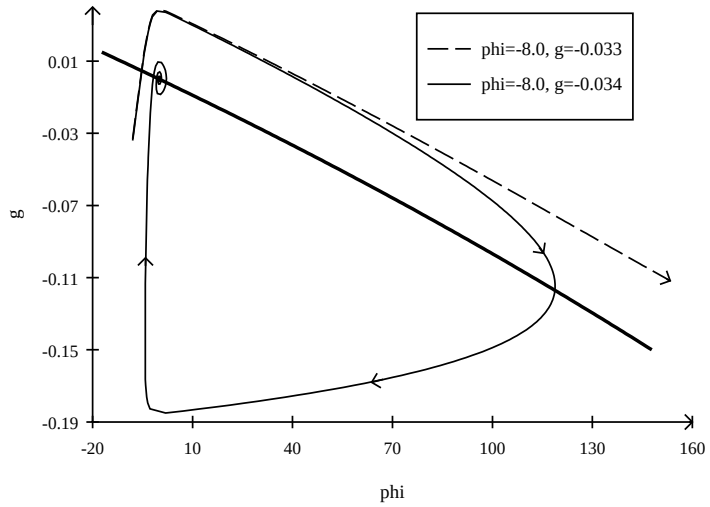

Figure 5: Trajectory Stability for $\tan\psi = 1$, $k = 3k_{cr}$. The stability boundary lies between the stable and unstable trajectories shown.

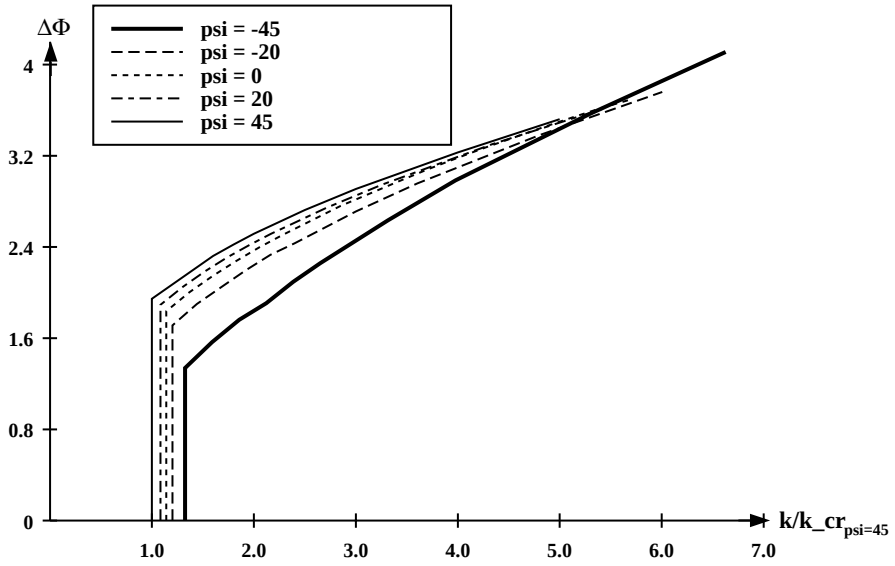

Figure 6: Maximum load-point velocity step $\Delta\phi$ as a Function of $k/k_{cr}(\psi = \pi/4)$ for Various Spring Angles (expressed in degrees). Based on maximum velocity overshoot of $\phi = 7$.

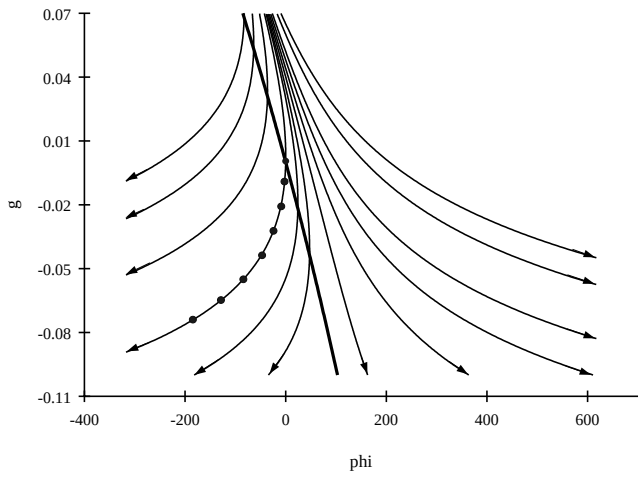

Figure 7: Stationary Load Point with $\tan\psi = 1$ and $k = 3k_{cr}$. The dotted trajectory is followed by the sliding block when the load-point, originally moving with velocity v_0, stops suddenly. Similar trajectories are obtained for other spring angles.

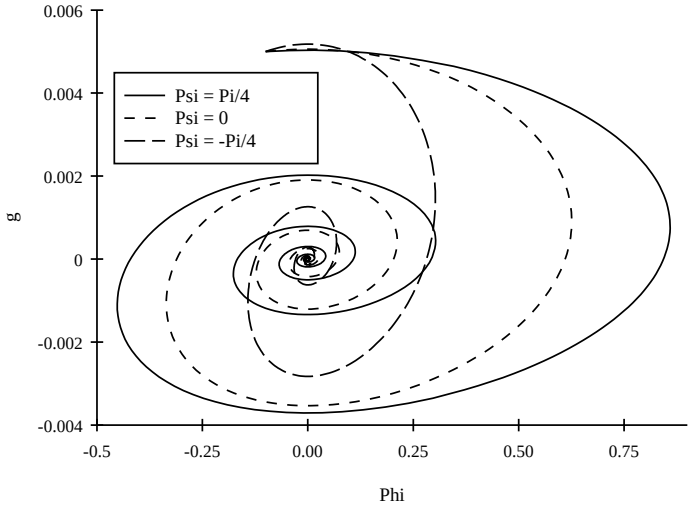

Figure 8: Comparison of Trajectories for Various ψ with Fixed $k > k_{cr}$.

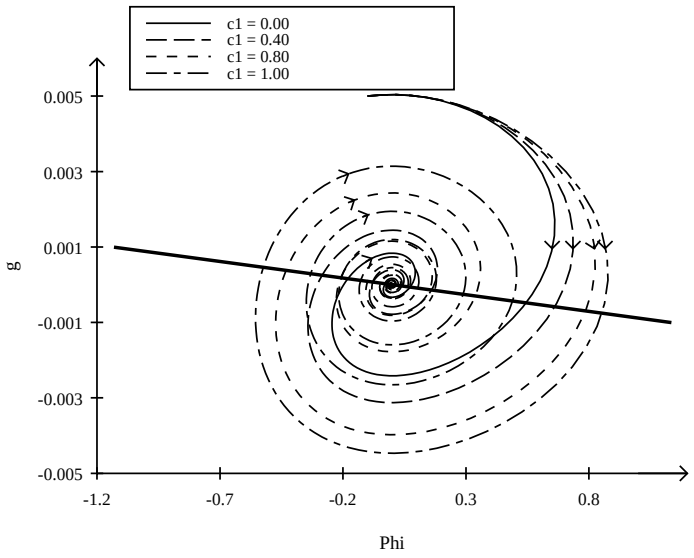

Figure 9: Effect of α for $\psi = \pi/4$. $c_1 = \alpha/\mu_{ss}$, $\mu_{ss} = 0.70$ and $k = 3k_{cr}$.

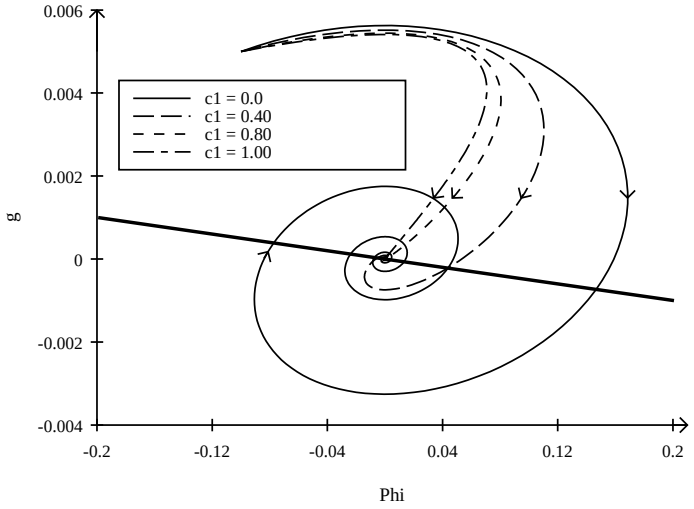

Figure 10: Effect of α for $\psi = -\pi/4$. $c_1 = \alpha/\mu_{ss}$, $\mu_{ss} = 0.70$ and $k = 3k_{cr}$.